Harmonic Distortion Prediction Method for a Meshed Transmission Grid with Distributed Harmonic Emission Sources – Eastern Danish Transmission Grid Case Study

Akhmatov, Vladislav; Sørensen, Mikkel; Jakobsen, Troels; Hansen, Chris Skovgaard ; Gellert, Bjarne Christian; Bukh, Bjarne Søndergaard

Published in:
Proceedings of 21st Wind & Solar Integration Workshop

Publication date:
2022

Document Version
Publisher's PDF, also known as Version of record

HARMONIC DISTORTION PREDICTION METHOD FOR A MESHED TRANSMISSION GRID WITH DISTRIBUTED HARMONIC EMISSION SOURCES – EASTERN DANISH TRANSMISSION GRID CASE STUDY

Vladislav Akhmatov[1], Mikkel Sørensen[1], Troels Jakobsen[1], Chris Liberty Skovgaard[1], Bjarne Christian Gellert[1], Bjarne Søndergaard Bukh[1,2]*

[1]*Energinet, Transmission System Operator of Denmark, Fredericia, Denmark*
[2]*AAU Energy, Aalborg University, Denmark*
**vla@energinet.dk*

Keywords: HARMONIC DISTORTION, MESHED TRANSMISSION GRID, UNDERGROUND CABLES, SIMULATION, VALIDATION

Abstract

Tremendous, fast green transition in Denmark initiates large-scale grid-integration of renewable energy sources, electrification of energy consumption, establishment of PtX and Energy Islands set goals for the transmission grid development, such as establishment of new connections, and grid reconstruction such as extensive substitution of overhead lines (OHL) with underground cables (UGC). The share of UGC in the Danish transmission grid is increasing. Presence of UGC has resulted in that resonances of the harmonic impedance characteristics of the transmission grid are brought within the harmonic order range coinciding with the harmonic distortion and causing systemwide increase of the harmonic voltage distortion in the 400 kV meshed transmission grid. Transformation of the 400 kV transmission grid arises needs of predicting the harmonic voltage distortion using simulation models to secure an adequate power quality and support investment decisions and harmonic mitigation for the grid stage which is not yet established and differs from the present grid. This paper presents a method of direct simulation of the harmonic voltage distortion, which is developed and applied by Energinet, Transmission System Operator of Denmark, using Eastern Danish 400 kV transmission grid as a case study. The main advantage of direct simulation is possibility to predict whether, where in the transmission grid, and for which harmonic orders, the not yet commissioned connections may cause violation of the IEC planning levels and which mitigation is necessary for bringing the harmonic distortion down below the planning levels with a given margin. Further, this paper briefly presents directions for the harmonic assessment in Denmark as part of an industrial PhD project by Energinet and Aalborg University. This joint work shall result in a guideline for prediction of the harmonic distortion in a meshed grid such as where and how an analytical approach can replace observational studies with many numerical simulations.

1 Abbreviations

DELFIN	SCADA of Energinet monitoring, gathering and processing the continuous electrical parameters, such as current, voltage and power, of the grid equipment in real time
DKE	Eastern Denmark (Transmission Grid)
DKW	Western Denmark (Transmission Grid)
ELVIS	Simulation model database of Energinet of the transmission grid for electricity
EL-POINT	SCADA of Energinet monitoring, gathering and processing the status of breakers and disconnectors of the grid components in real time
HVAC	High Voltage Alternating Current
HVDC	High Voltage Direct Current
LCC	Line Commutated Converter
OHL	Overhead Line
OWPP	Offshore Wind Power Plant
POE	Point of Evaluation
PQ	Power Quality
PV	Photovoltaic
SAFIR	Power quality monitoring, gathering and processing system of Energinet (in this context)
SCADA	Supervisory Control and Data Acquisition
SE4	Market Zone 4 of the transmission grid of Sweden
SG	Synchronous Generator
SvK	Svenska Kraftnät, Transmission System

This paper "Harmonic Distortion Prediction Method for a Meshed Transmission Grid with Distributed Harmonic Emisssion Sources - Eastern Danish Transmission Grid Case Study" was presented at the 21st Wind & Solar Integration Workshop and published in the workshop's proceedings.

	Operator of Sweden
VSC	Voltage Source Converter
UGC	Underground Cable

1.1 HVAC substations

The 400 kV substations in Eastern Denmark.

ASV	Asnæs	HCV	H C Ørsted Værket
AVV	Avedøre	HKS	Herslev
BJS	Bjæverskov	HVE	Hovegård
GLN	Glentegård	ISH	Ishøj
GØR	Gørløse		

The 132 kV substations in Eastern Denmark with relevance for the presentation.

AMV	Amager	HCV	H C Ørsted Værket
ASV	Asnæs	HVE	Hovegård
AVV	Avedøre	ISH	Ishøj
BJS	Bjæverskov	RAD	Radsted
GLN	Glentegård	RIN	Ringsted
GØR	Gørløse	TEG	Teglstrupgård
		VAL	Valseværket

The 400 kV substations in Sweden with relevance for the presentation.

SÅNS	Söderåsen	AIES	Aries
LDOS	Lindome	STÖS	Stärnö
RINS	Ringhals	STRS	Strömma
MIDS	Midskog		

The 132 kV substations in Sweden with relevance for the presentation.

LDOS	Lindome	MRPS	Mörap
LILS	Lillgrund	SEES	Sege

1.2 HVDC Connections and Converter Stations

The HVDC converter stations in Eastern Denmark (LCC).

KO	Kontek (600 MW, BJS, DKE – Germany)
SB	Storebælt (600 MW, HKS, DKE – DKW)

The HVDC converter stations in Sweden with relevance for the presentation (LCC).

BA	Baltic Cable (600 MW, AIES, Sweden – Germany)
KS1	Konti-Skan 1 (370 MW, LDOS 400 kV, Sweden – DKW)
KS2	Konti-Skan 2 (370 MW, LDOS 132 kV, Sweden – DKW)
SP	SwePol (600 MW, STÖS, Sweden – Poland)

2 Introduction

Tremendous, accelerated green transition of the energy sectors implies, on the one hand, a greater level of renewable energy utilization within electric energy production, consumption, transportation, heating and storing instead of fossil energy sources and, on the other hand, a necessity of expansion and reconstruction of the transmission grid. The green transition may, on the one hand, introduce evolution of the harmonic emission sources including more converter-interfaced units within energy supply, storage, consumption, and transportation, and, on the other hand, development, reinforcement, and reconstruction of the electricity infra-structure altering the harmonic impedance characteristics and resonances of the transmission grid. Securing adequate power quality and mitigation of excessive harmonic voltage distortion is a necessity for successful green transition and development of the transmission grid. Ability to predict the harmonic voltage distortion in a future grid using validated simulation models and proposal of harmonic mitigation are important goals for the grid analysis and development.

Direct simulation of the harmonic voltage distortion in the meshed transmission grid is a complex matter. The transmission grid can be in different operation conditions, implying some connections and shunts being out-of-service. The harmonic emission sources are harmonic vectors with magnitudes, phase-angles and, though, phase asymmetry [1]. Superposition of the harmonic vectors may increase the background harmonic voltage distortion in one part of the meshed transmission grid and reduce the distortion in another part [2], which depends on the harmonic impedance characteristics of the grid being in certain operation conditions. Therefore, direct simulation of the harmonic voltage distortion requires both passive-grid data such as OHL, UGC, transformers and shunts, and the data of harmonic emission sources such as harmonic vectors using Norton and Thevenin equivalents [3].

Usually, electrical and geometrical data of the OHL, UGC, transformers and shunts can be acquired and validated by measurements with accuracy and detail sufficient for calculations of the harmonic impedance characteristics. Such calculations are conducted using the frequency sweeps. The frequency sweeps are a tried-and-proven method and present in many commercially available simulation programs for the grid analysis. The frequency sweeps will produce the harmonic impedance characteristics and identify harmonic resonances, or just the harmonic orders with large impedance magnitudes, as the ability of the grid to increase the harmonic voltage distortion in coincidence with the harmonic emission sources. However, the frequency sweeps do not predict whether and to which extent the harmonic voltage distortion will increase because this method does not account for harmonic emission sources. In other words, a harmonic resonance may amplify the harmonic voltage distortion in a certain part of the grid if there are harmonic emission sources

exciting this resonance. If there are no such distortion (no sources), then there is nothing to amplify.

Factual magnitudes of the harmonic emission may differ from the worst-case magnitudes depending on the grid operation conditions and vectoral superposition of the harmonic emission under the substations [1]. For simulation of the harmonic voltage distortion, additional numerical work shall be done for identification of such magnitudes and phase-angles of the harmonic sources under the substations.

Energinet has developed a deterministic method for representation of the harmonic emission sources in the meshed transmission grid and applies this method for direct simulation of the harmonic voltage distortion. The deterministic method is successfully validated by the PQ measurements of the present-stage grid in different (n-L), $L \geq 0$, operation conditions. The deterministic method allows prediction of the harmonic voltage distortion in the transmission grid after commissioning of a new connection or replacement of an existing OHL with UGC.

This paper will present the deterministic method for simulation and prediction of the harmonic voltage distortion developed by Energinet using the Eastern Danish 400 kV transmission grid as a case study. This paper will demonstrate accuracy of the method using validation cases in different (and often challenging) operation conditions of the transmission grid. The paper will also make a short introduction to an ongoing joint work of Energinet and Aalborg University with analytical assessment of the harmonic distortion in the meshed transmission grid.

3 Developing Electricity Infrastructure

Specifically for Denmark, principles for developing the electricity infrastructure have been defined in the political agreement from October 2020:

- New 400 kV transmission lines must be established as UGC to the extent that is technically feasible. Beyond what is technically feasible to establish with UGC, OHL must be used for 400 kV lines.
- Existing 132-150 kV OHL are replaced with UGC as the need for extensive reinvestment of the lines arises. Furthermore, existing 132-150 kV OHL are replaced with UGC if the lines are in the vicinity of new 400 kV OHL.
- New 132-150 kV transmission lines are established as UGC.

The share of UGC in the meshed transmission grid is increasing which brings the harmonic resonances down within the harmonic order ranges coinciding with the harmonic emission sources. For the Danish 400 kV transmission grid, the characteristic harmonic orders are the 3rd, 5th, 7th, 11th, 13th, 23rd and 25th. Considering the power quality issues versus UGC utilization, the Danish experience so far is presented below followed by marking in Fig. 1.

Energization of the relatively short, about 7 km system length, 400 kV double UGC system of Vejle-Ådal in July 2017 in Western Denmark, leads to a significant amplification of the 11th and 13th harmonic voltage distortion in the 400 kV grid areas about 80 km away from Vejle-Ådal [4]. The topic of harmonic amplification becomes a concern for further cabling projects in Denmark and defining a goal for development of a simulation model for prediction of the harmonic voltage distortion in the meshed transmission grid of Denmark validated by measurements. Simulation of the Vejle-Ådal UGC is given in Appendix A.

Energization of a new 400 kV OHL connection between the substation Kassø in Western Denmark (Southern Jutland) and the substation Handewitt in Germany in July 2020 is followed by an increase of the 11th (and 13th) harmonic voltage distortion in Eastern Jutland about 40 km away from Kassø. At this time, a simulation model for harmonic assessment of the 400 kV transmission grid in Western Denmark has become available. The simulation model, which is empirically developed and validated by PQ measurements, has reached to the same conclusion on a slight increase of the 11th (and 13th) harmonic voltage distortion in Eastern Jutland after enabling the 400 kV OHL connection between Kassø and Handewitt.

The 5th harmonic voltage distortion in the 150 kV substation Stovstrup in Western Denmark used to exceed the IEC planning level. The harmonic assessment by simulations for the 150 kV grid-reconstruction replacing the OHL with UGC between the substations Kassø and Ribe in Western Denmark has predicted reduction of the excessive 5th harmonic voltage distortion in Stovstrup down below the IEC planning level [2]. The substation Stovstrup is located about 90 km from the assessed 150 kV grid-reconstruction project. This reduction of the 5th harmonic voltage in Stovstrup is now confirmed by measurements after the first overhead lines between Kassø and Ribe are replaced with the UGC in November 2021.

The harmonic assessment by simulations for the Revsing-Landerupgård 400 kV connection by 2027, approx. 25 km system length, has shown that the full UGC connection will cause a smaller increase of the harmonic voltage distortion than the full OHL connection in Western Denmark. This outcome is explained through the harmonic propagation between the Western and Eastern 400 kV backbone systems of Western Denmark with uncorrelated harmonic voltage distortion, which becomes linked via the Revsing-Landerupgård 400 kV connection, and the differences in the harmonic impedance imposed by the UGC in comparison to the OHL.

The harmonic assessment by simulations for the Kongernes Nordsjælland 400 kV UGC connection, approx. 11 km system length, replacing OHL in Eastern Denmark by 2026 has predicted significant increase of the 7th harmonic voltage distortion in areas located approx. 30 ...40 km away from the assessed UGC connection. The results are explained by harmonic resonance shifts in the meshed 400 kV grid of Eastern Denmark [5].

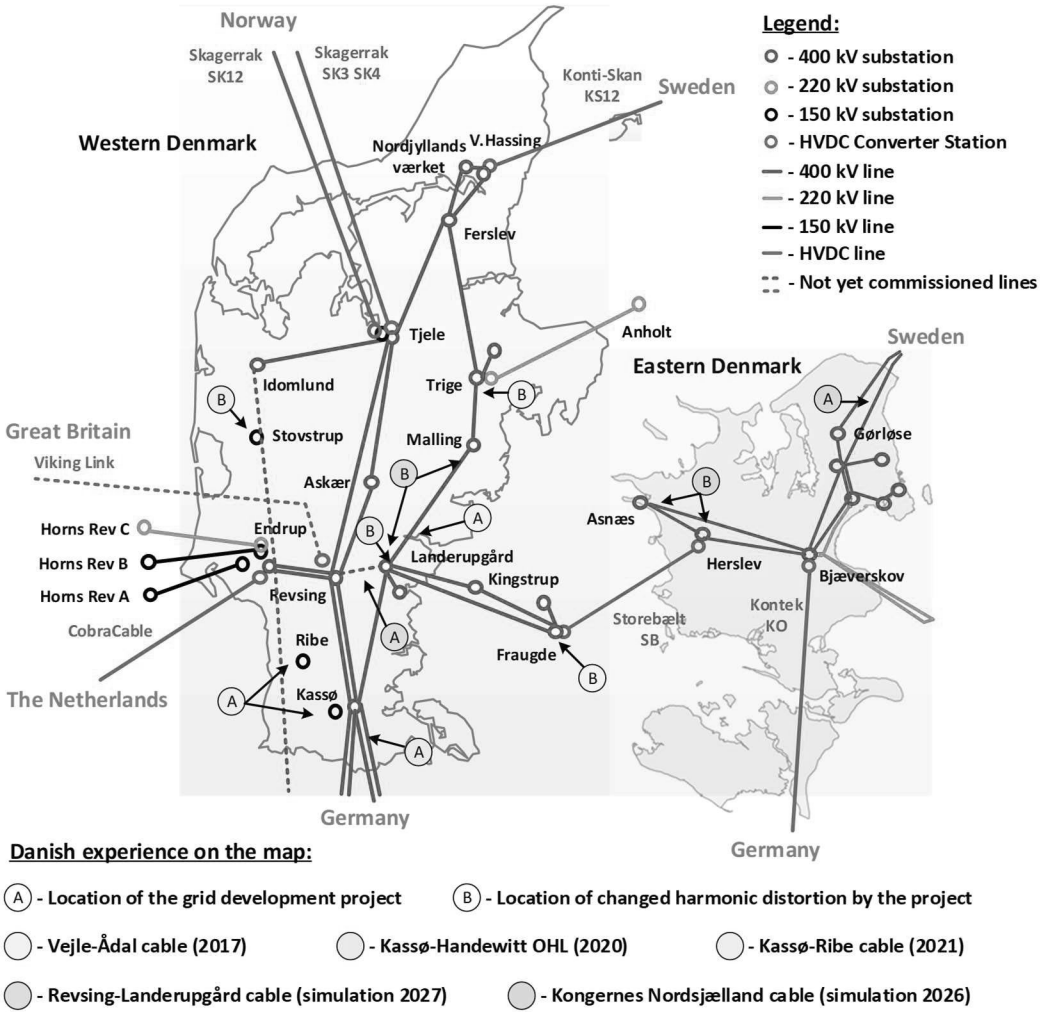

Fig. 1 400 kV transmission grid of Denmark (2021) with marking of the grid development projects and areas of their impact on harmonic distortion

The Danish experience so far confirms complexity of analyzing the power quality issues in the meshed transmission grid which may occur after grid reinforcements and new UGC connections. The experience also confirms a necessity of sufficiently accurate and validated simulation models of the meshed transmission grid with multiple sources for conducting harmonic assessment.

4 Method

The standardized analytical modelling methods are developed and successfully validated for radial connections with a single harmonic emission source in the one end and a POE in the other end of the radial connection. However, the transmission grid is meshed and includes multiple harmonic emission sources. To our knowledge, there is no publicly available, proven by PQ measurements, analytical method for preparation of such simulation models for meshed transmission systems with multiple harmonic emission sources. The presented simulation model for harmonic assessment of the meshed transmission grid is deterministic, i.e. empirically developed.

In the deterministic model, the harmonic emission sources are Norton equivalents with the harmonic current vectors, J_N, where N is the source id. The harmonic current vectors J_N propagate between the substations via the impedances Z_{NM} and induce the harmonic voltages in the substations, U_M, where M is the substation id. When the Thevenin equivalents are included, these are mathematically converted into the Norton equivalents for simplicity of this presentation. The model equations become:

$$\begin{bmatrix} U_1 \\ U_2 \\ \vdots \\ U_M \end{bmatrix} = \begin{bmatrix} Z_{11} & Z_{12} & \cdots & Z_{1N} \\ Z_{21} & Z_{22} & \cdots & Z_{2N} \\ \vdots & \vdots & \ddots & \vdots \\ Z_{M1} & Z_{M2} & \cdots & Z_{MN} \end{bmatrix} . \begin{bmatrix} J_1 \\ J_2 \\ \vdots \\ J_N \end{bmatrix} \quad , \qquad (1)$$

where the impedances Z_{MN} couple the simulated harmonic voltage distortion U_M in the substation M with the simulated harmonic current emission J_N of the source id N. The impedances Z_{MN} are in complex numbers, the harmonic voltages U_M and harmonic currents J_N are vectors (complex numbers) with magnitudes and phase-angles [2].

The impedance matrix $[Z_{MN}]$ of Eq. (1) is known with sufficient confidence from the electrical and geometrical data

of the passive-grid components such as OHL, UGC, transformers and shunts.

The harmonic emission sources are defined by their locations in the grid, harmonic orders, harmonic magnitudes and harmonic phase-angles. This method works with the two types of the harmonic emission sources:

- Vendor specific sources.
- Distributed harmonic sources.

The vendor-specific sources representing the HVDC Converter Stations are available and include specific locations in the grid, harmonic orders and worst-case magnitudes as nonlinear dependencies of the power transport and direction, i.e. rectifier or inverter operation of the HVDC Converter Station. The harmonic phase-angles to be assigned to the current source at the HV terminal, are not available from the data.

For the distributed harmonic sources, the harmonic magnitudes or phase-angles are not readily available. Hence the locations in the grid and harmonic orders are only identifiable using the PQ measurements. Thus, the harmonic magnitudes and phase-angles of the harmonic current sources $J_1 \ldots J_N$ in Eq. (1) in detail being necessary for harmonic assessment are unknown from the data.

The measured harmonic voltage magnitudes, $|U_M|$, are available for majority of the 400 kV substations year around. The harmonic phase-angles are not included in the PQ measurements.

From the above discussion it becomes clear that the number of unknown variables, meaning unknown magnitudes and phase-angles, exceeds the number of linear equations of Eq. (1). Analytical unambiguous solution of Eq. (1) for finding the harmonic current vectors $J_1 \ldots J_N$ does not seem possible [2].

Instead, the deterministic method is applied so that the numerical tuning of the magnitudes and phase-angles of the harmonic current vectors results in the harmonic load-flow solution by Eq. (1) to converge toward the measured harmonic voltage magnitudes [2]. The numerical tuning is simultaneously conducted for several grid operation conditions combining the various power transports and filter utilizations of the HVDC Converter Stations with the (n-L), $L \geq 0$, conditions referring to the 400 kV transmission lines and power transformers.

Inclusion of the various grid operation regimes with the (n-L) conditions implies that the impedance matrix $[Z_{MN}]$ varies. This variation corresponds to the different but specific magnitudes of the measured harmonic voltage magnitudes $|U_M|$ in the substations. The target of the numerical tuning is to define an (empirically developed) solution set of the harmonic current sources $J_1 \ldots J_N$ complying with the specific magnitudes of the measured harmonic voltages $|U_1| \ldots |U_M|$ for the specific impedance matrix variations:

$$\begin{cases} \begin{bmatrix} U_1 \\ U_2 \\ \vdots \\ U_M \end{bmatrix}_{OC\_1} = \begin{bmatrix} Z_{11} & Z_{12} & \cdots & Z_{1N} \\ Z_{21} & Z_{22} & \cdots & Z_{2N} \\ \vdots & \vdots & \ddots & \vdots \\ Z_{M1} & Z_{M2} & \cdots & Z_{MN} \end{bmatrix}_{OC\_1} \cdot \begin{bmatrix} J_1 \\ J_2 \\ \vdots \\ J_N \end{bmatrix}, \\ \begin{bmatrix} U_1 \\ U_2 \\ \vdots \\ U_M \end{bmatrix}_{OC\_2} = \begin{bmatrix} Z_{11} & Z_{12} & \cdots & Z_{1N} \\ Z_{21} & Z_{22} & \cdots & Z_{2N} \\ \vdots & \vdots & \ddots & \vdots \\ Z_{M1} & Z_{M2} & \cdots & Z_{MN} \end{bmatrix}_{OC\_2} \cdot \begin{bmatrix} J_1 \\ J_2 \\ \vdots \\ J_N \end{bmatrix}, \\ \vdots \\ \begin{bmatrix} U_1 \\ U_2 \\ \vdots \\ U_M \end{bmatrix}_{OC\_K} = \begin{bmatrix} Z_{11} & Z_{12} & \cdots & Z_{1N} \\ Z_{21} & Z_{22} & \cdots & Z_{2N} \\ \vdots & \vdots & \ddots & \vdots \\ Z_{M1} & Z_{M2} & \cdots & Z_{MN} \end{bmatrix}_{OC\_K} \cdot \begin{bmatrix} J_1 \\ J_2 \\ \vdots \\ J_N \end{bmatrix}, \end{cases} \quad (2)$$

where the index OC denotes the total of K operation conditions with the id from 1 to K.

First, the above-described method increases the number of equations with unchanged number of the unknown variables, i.e. the harmonic current magnitudes and harmonic phase-angles. Therefore, this method increases the odds for converging toward the (empirically defined) solution set of the magnitudes and phase-angles of the harmonic current sources $J_1 \ldots J_N$.

Second, the solution set of the harmonic current sources will comply with the various (n-L) operation conditions of the passive-part of the transmission grid, with $L \geqslant 0$. Interpreting the grid development project as (n-L_1+L_2) with L_1 denoting the number of removed lines and L_2 the number of new lines, the solution set of the harmonic current sources $J_1 \ldots J_N$ shall simulate the harmonic voltage distortion in the grid after commissioning of the grid reinforcement so that introducing a new operation condition OC_(K+1) → (n-L_1+L_2):

$$\begin{bmatrix} U_1 \\ U_2 \\ \vdots \\ U_M \end{bmatrix}_{(n-L1+L2)} = \begin{bmatrix} Z_{11} & Z_{12} & \cdots & Z_{1N} \\ Z_{21} & Z_{22} & \cdots & Z_{2N} \\ \vdots & \vdots & \ddots & \vdots \\ Z_{M1} & Z_{M2} & \cdots & Z_{MN} \end{bmatrix}_{(n-L1+L2)} \cdot \begin{bmatrix} J_1 \\ J_2 \\ \vdots \\ J_N \end{bmatrix}. \quad (3)$$

Thus, the presented deterministic method shall allow direct simulation of the harmonic voltage distortion in the next, not yet commissioned, grid expansion stage applying the validated by measurements representations of the harmonic emission sources in the present stage grid:

$$\begin{bmatrix} U_1 \\ U_2 \\ \vdots \\ U_M \end{bmatrix}_{NEXT} = \begin{bmatrix} Z_{11} & Z_{12} & \cdots & Z_{1N} \\ Z_{21} & Z_{22} & \cdots & Z_{2N} \\ \vdots & \vdots & \ddots & \vdots \\ Z_{M1} & Z_{M2} & \cdots & Z_{MN} \end{bmatrix}_{NEXT} \cdot \begin{bmatrix} J_1 \\ J_2 \\ \vdots \\ J_N \end{bmatrix}_{PRESENT}. \quad (4)$$

4.1 Relative magnitudes and phase-angles

Direct simulation of the harmonic voltage distortion in the transmission grid in various operation conditions as well as prediction in a future grid implies that the harmonic magnitudes and phase-angles of the empirically defined solution set are not changed. The same, locked, magnitudes and phase-angles of the solution set shall produce the closest possible match between the simulated and measured harmonic voltage magnitudes in the substations of the present grid stage at (n-L), $L \geq 0$, for securing applicability of the

same solution set for prediction of the harmonic voltage distortion in the next grid expansion stage (n-L_1+L_2).

Intuitively, the above statement may seem contradicting with observations that the harmonic magnitudes and phase-angles of the measured harmonic current are varying in time. The above stated observation is correct referring to that absolute magnitudes and phase-angles of the harmonic current vectors vary in time. In the presented method, the relative magnitudes and relative phase-angles are locked and kept unchanged whereas the absolute values may vary between the different operation conditions of the transmission grid.

The relative magnitudes of the harmonic current vectors in the three phases $J^{R}_{A\_h}$, $J^{R}_{B\_h}$, and $J^{R}_{C\_h}$, are the absolute harmonic magnitudes J_{A_h}, J_{B_h}, and J_{C_h}, with reference to the nominal-frequency magnitudes, J_{A_1}, J_{B_1}, and J_{C_1}:

$$\frac{J_{A\_h}(A)}{J_{A\_1}(A)} = J^{R}_{A\_h},\ \frac{J_{B\_h}(A)}{J_{B\_1}(A)} = J^{R}_{B\_h},\ \frac{J_{C\_h}(A)}{J_{C\_1}(A)} = J^{R}_{C\_h}. \quad (5)$$

The relative phase-angles $\alpha^{R}_{A\_h}$, $\alpha^{R}_{B\_h}$, and $\alpha^{R}_{C\_h}$ are defined from the absolute phase-angles of the harmonic current vectors, φ_{A_h}, φ_{B_h}, and φ_{C_h}, with reference to the nominal-frequency phase-angles, φ_{A_1}, φ_{B_1}, and φ_{C_1}:

$$\begin{aligned} \varphi_{A\_h} - h \cdot \varphi_{A\_1} &= \alpha^{R}_{A\_h}, \\ \varphi_{B\_h} - h \cdot \varphi_{B\_1} &= \alpha^{R}_{B\_h}, \\ \varphi_{C\_h} - h \cdot \varphi_{C\_1} &= \alpha^{R}_{C\_h}. \end{aligned} \quad (6)$$

Thus, each harmonic emission source for each harmonic order, h, is defined by the four constants C_{1h}, C_{2h}, C_{3h} and C_{4h}. The three first constants define the relative harmonic magnitudes:

$$J^{R}_{A\_h} = C_{1h},\ J^{R}_{B\_h} = C_{2h},\ J^{R}_{C\_h} = C_{3h}. \quad (7)$$

Application of the three constants (instead of one) allows representation of asymmetry between the harmonic phase currents [1] of the harmonic order h. The fourth constant defines the relative harmonic phase-angles in relation to symmetrical components according to:

$$\begin{aligned} \alpha^{R}_{A\_h} &= C_{4h}, && h = 4, 7, 10, 13 \ldots \\ \alpha^{R}_{B\_h} &= C_{4h} \pm \frac{2}{3}\pi, && \begin{cases} h = 2, 5, 8, 11 \ldots \\ h = 3, 6, 9, 12 \ldots \end{cases} \\ \alpha^{R}_{C\_h} &= C_{4h} \mp \frac{2}{3}\pi, && \begin{cases} h = 2, 5, 8, 11 \ldots \\ h = 3, 6, 9, 12 \ldots \end{cases} \end{aligned} \quad (8)$$

The numerical tuning of Eq. (2) shall converge to the (empirically defined) solution set where the relative magnitudes by Eq. (5) and relative phase-angles by Eq. (6) remain constant for all operation conditions of the grid (n-L), $L \geq 0$, and power transports of the HVDC Converter Stations. The numerical tuning of the harmonic emission sources and determination of the four constants, C_{1h}, C_{2h}, C_{3h} and C_{4h}, have been done manually so far, including the results of [1], [2], [5] and this presentation. The numerical tuning is conducted simultaneously for all harmonic emission sources and operation conditions, which makes a heavy process. At present, Energinet tests an automated, fast converging, method for the numerical tuning of the harmonic emission sources.

4.2 Preconditions and precautions

For the harmonic distortion prediction, the important precondition is that the grid development project shall not introduce new harmonic emission sources which are able significantly to disturb the accuracy of the numerical solution of Eq. (3).

The grid development project corresponds to a change of the impedance matrix $[Z_{NM}]$. The important precondition of applying Eq. (3) is that the grid development project is commissioned within the geographical area of the original impedance matrix $[Z_{NM}]$ applied for developing the solution set $J_1 \ldots J_N$.

Violation of the above given preconditions may result in miscalculation of the harmonic voltage distortion in the next grid expansion stage.

The frequency sweeps shall always be conducted together with direct simulation of the harmonic voltage distortion as part of the harmonic assessment. The results and conclusions of the direct simulation of the harmonic voltage distortion by the above-described method and those of the frequency sweeps shall support one another to form solid conclusions.

When the grid development project is completed and taken into service, the simulation model shall be re-validated. The new connection data shall be validated by measurements and applied as-built in the passive-part grid model. Then, the simulated harmonic voltage distortion shall be compared to the PQ measurements for the new grid stage. In discrepancy, the empirically defined solution set of the harmonic emission sources shall be readjusted according to the above-described method.

5 Transmission Grid of Eastern Denmark

The transmission grid of Eastern Denmark (DKE including the islands of Zealand, Lolland, Falster and Moen) is synchronous with the Nordic Countries and asynchronous with the Continental Europe, meaning asynchronous with the transmission grid of Western Denmark (DKW including the peninsula of Jutland and the island of Funen). The DKE transmission grid includes the 400 kV, 220 kV (onshore and offshore) and 132 kV meshed grids.

The 400 kV transmission grid is the backbone of the DKE transmission grid and stylistically drawn in Fig. 2. DKE is HVAC connected to Sweden via the two 400 kV and the two 132 kV combined OHL and submarine cable connections. The two 400 kV connections to Sweden are between the substations Gørløse (GØR) and Hovegård (HVE) in DKE and Söderåsen (SÅNS) in Sweden. The two 132 kV connections are between the substation Teglstrupgård (TEG) in DKE and Mörap (MRPS) in Sweden.

DKE is HVDC connected to Germany via the Kontek (KO) HVDC LCC connection and to DKW via the Storebælt (SB) HVDC LCC connection. Each HVDC connection is with 600 MW rating Converter Stations. DKE is also connected to Germany via the 220 kV cables, 220/150 kV offshore transformation, 150 kV cables and the Back-to-Back VSC Converter Station in Bentwisch (400 MW, Germany) of the Kriegers Flak Combined Grid Solution.

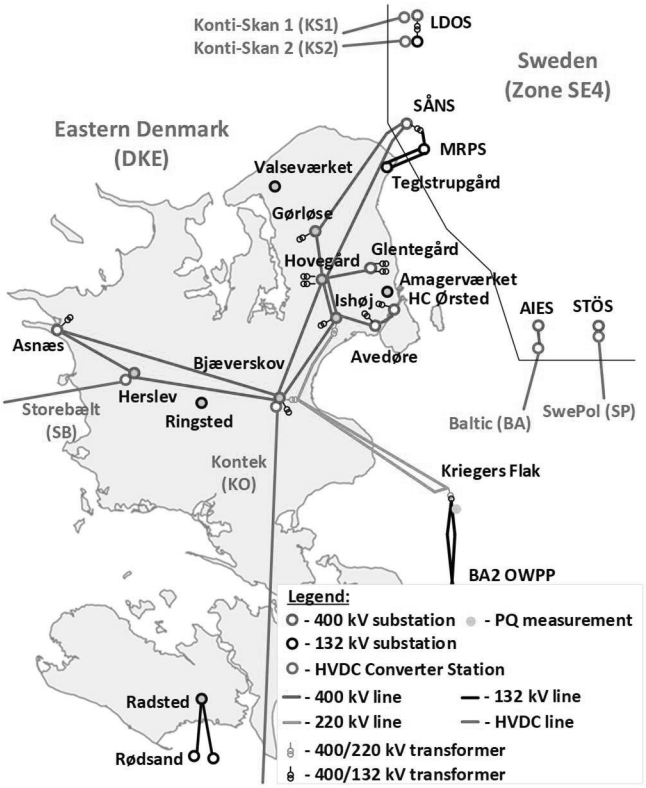

Fig. 2 400 kV transmission grid of Eastern Denmark (2021) with connection to and HVDC Converter Stations in Sweden Zone SE4.

The Swedish Market Zone SE4 is in proximity of the DKE transmission grid and includes the 400 kV and 132 kV meshed transmission grids and several HVDC connections to the foreign systems. The SE4 transmission grid is HVDC connected to DKW via the Konti-Skan HVDC LCC connections (740 MW in total), to Germany via the Baltic Cable HVDC LCC connection (600 MW) and to Poland via the SwePol HVDC LCC connection (600 MW). At the internal border, SE4 is HVAC connected to the Swedish Market Zone 3. Due to proximity and strong electrical coupling of the 400 kV transmission grids of DKE and SE4, both grids are part of the simulation model for harmonic assessment of the DKE 400 kV transmission grid.

6 Simulation Model Development Process

The development process of the model for direct simulation of the harmonic voltage distortion is shown in Fig. 3. The process includes the three major steps.

The first step is grid data and measurements acquisition and processing. This shall result in time synchronized data combining the PQ measurements, the measured power transports of the HVDC Converter Stations and grid operation conditions (n-L), $L \geq 0$. The time synchronized data are divided into the periods and snapshots to be used for numerical tuning of the harmonic emission sources and validation of the simulation model.

Each period includes several consecutive snapshots so that not only the stationary magnitudes but also changes and steps of the harmonic voltage distortion due to changes of the grid operation conditions are represented and validated in the simulation model. In the presented work, seven periods with durations of several days, are selected over a year and four months in 2020-2021. The periods are divided into sixty consecutive snapshots and applied for the model development and validation. The periods include various and changing operation conditions, with up to (n-5) in the 400 kV transmission grid and the HVDC transports from none up to the full capacity. The out-of-service components counted as (n-L) events include the 400 kV transmission lines and 400/132 kV transformers in Eastern Denmark.

The (n-L), $L \geq 0$, operation conditions represent changes within the harmonic impedance matrix according to Eq. (1-2). Thus, these conditions define the area of the transmission grid where the developed model is applicable for simulation of the harmonic voltage distortion in response to changes of the harmonic impedance matrix. The (n-L) events are marked by arrows in Fig. 4. By inspection of the area with such (n-L) events in Fig. 4, the developed model for direct simulation of the harmonic voltage distortion is applicable within the entire 400 kV transmission grid of Eastern Denmark (the present stage grid).

The second step is preparation of the passive-part grid model including the geometrical and electrical data of the transmission lines, power transformers and shunts. These data are acquired using the ELVIS database of Energinet and the data received from the cable vendors and validated from the (nominal-frequency) impedance measurements.

The third step is definition and numerical tuning of the harmonic emission sources according to Eq. (1) resulting in an empirically defined solution set of the harmonic current and voltage vectors implying the set of relative magnitudes and relative phase-angles according to Eq. (5-8). The relative magnitudes and relative phase-angles of the harmonic current and voltage vectors shall match the measured harmonic voltage distortion in the 400 kV substations in as many as possible grid operation conditions by the snapshots.

The locations of the harmonic emission sources in the simulation model are shown in Fig. 4.

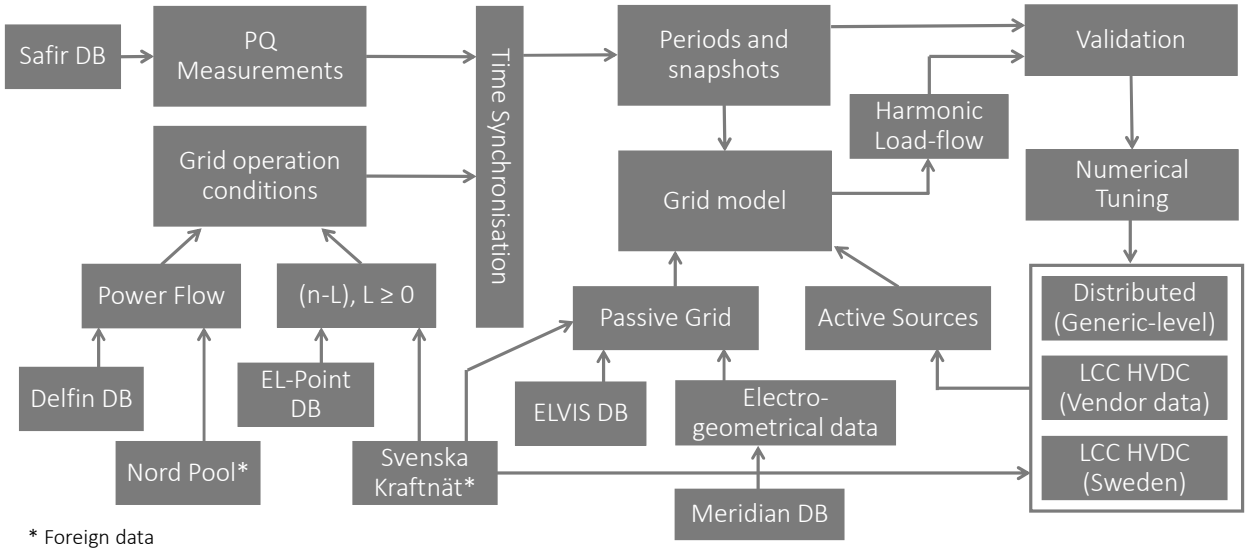

Fig. 3 Development process of the model for direct simulation of harmonic voltage distortion in 400 kV transmission grid of Eastern Denmark

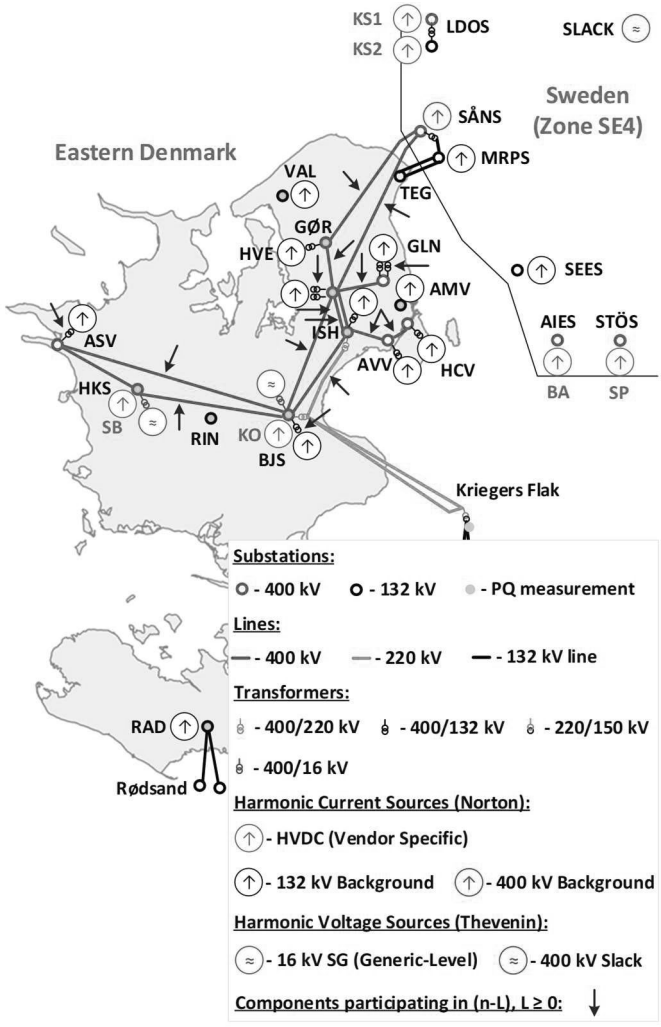

Fig. 4 400 kV transmission grid of Eastern Denmark (2021) with marking of the harmonic emission source models and passive-grid components participating in (*n-L*) events for the simulation model development.

The harmonic emission sources representing the HVDC Converter Stations are in their grid-connection substations, such as BJS for Kontek and HKS for Storebælt in DKE, and LDOS for Konti-Skan 1 and 2, AIES for Baltic and STÖS for SwePol in Sweden.

The distributed harmonic emission sources are physically located under the 132 kV substations. Their cumulative contributions to the harmonic voltage distortion in the 400 kV transmission grid are seen through the substations with 400/132 kV transformation. Therefore, the distributed harmonic emission sources are represented as the harmonic Norton equivalents in the 132 kV substations with 400/132 kV transformation. Since the 132 kV grid is meshed, the harmonic Norton equivalents are interconnected via the 132 kV grid.

More unit-specific, distinguishing, representation of the distributed harmonic emission sources under the 132 kV meshed transmission grid requires significantly more PQ measurements in the 132 kV substations than in the present grid stage, referring to Fig. 4. With only few PQ measurements, the model by Eq. (1) is underdefined because the number of equations significantly exceeds the number of the known (measured) variables, which is not possible to resolve (not without establishing more PQ measurements in the 132 kV substations).

The harmonic emission of the synchronous generators (SG) in the HVDC Converter Stations has marginal contributions, which however have been accounted for in the model using the Thevenin equivalents.

PQ measurements in Sweden are not available for development of the simulation model of Eastern Denmark. Therefore, the harmonic distortion exchanged via the HVAC cables with the Swedish transmission grid is seen in the Danish grid as cumulative harmonic emission of distributed sources behind the border substations SÅNS and MRPS

superimposed with the harmonic emission of the HVDC Converter Stations in Sweden: BA, KS1, KS2 and SP, the Lillgrund wind power plant (SEES) and the slack bus in SE3.

It is not possible to assign the harmonic emission sources to specific substations in the Swedish transmission grid without having access to the PQ measurements and grid operation conditions. Therefore, the developed simulation model is not applicable for simulation of the harmonic voltage distortion in specific substations of the Swedish transmission grid.

When the validation is completed, the relative magnitudes and relative phase-angles are locked, i.e. not permitted to be changed, and the empirically defined solution set of the harmonic emission sources is ready for direct simulation of the harmonic voltage distortion in the present grid stage and prediction of the harmonic voltage distortion in a future stage grid [5].

Already in the present stage grid, the PQ measurements are not installed in all 400 kV substations and there can be periods with unavailable PQ measurements in a single substation with the measurement equipment. The simulation model "fills out" missing measurements in such substations with the simulated magnitudes of the harmonic voltage distortion, so that catching potential power quality issues (already in the present stage grid).

6.1 Time-synchronization with sampled time

The PQ measurements are acquired from SAFIR as 10-minute samplings [3]. Therefore, the measured harmonic voltage magnitudes are 10-minute averages of the instant harmonic phase-to-ground voltage magnitudes.

The status of the breakers and disconnectors, such as going in-service or out-of-service, are acquired from EL-POINT in real-time, which implies reported immediately from the monitored device to EL-POINT. Therefore, 10-minute time sampling of the device status acquired from EL-POINT is made for synchronization with the time sampling of SAFIR.

The sampling instances of the PQ measurements in the different substations are mutually synchronised in SAFIR. However, the start and end time of the 10-minute averaging periods are not necessarily synchronized in the different substations. The last-mentioned desynchronization may introduce an inconsistency up to ± 10 minutes around the sampling instance when directly comparing the measured harmonic voltage magnitudes in different substations acquired from SAFIR and around the sampling instances of the component statuses acquired from EL-POINT and power transports from DELFIN.

The method of direct simulation of the harmonic voltage distortion applies harmonic load-flow, which per definition is a steady-state simulation. In the event of a grid component switches in- or out-of-service or an HVDC Converter Station ramps power, the harmonic voltage distortion transits between the two steady-state conditions, i.e. before and after the changed operation. Whether the measured harmonic voltage distortion, U_H, at the sampling instance, t_S, is in steady-state and applicable for validation of the simulated harmonic voltage distortion considers the above-described desynchronization within the period $\Delta t = \pm 10$ minutes around the sampling instance t_S using the three values:

- The minimum confidence range:
  $U_{H\_MIN}(t_S) = min(U_H(t_S-\Delta t), U_H(t_S), U_H(t_S+\Delta t))$.
- The maximum confidence range:
  $U_{H\_MAX}(t_S) = max(U_H(t_S-\Delta t), U_H(t_S), U_H(t_S+\Delta t))$.
- The average value:
  $U_{H\_AVE}(t_S) = (U_H(t_S-\Delta t)+U_H(t_S)+ U_H(t_S+\Delta t))/3$.

Demonstration of the time-synchronization algorithm is given in Fig. 5 for the measured 7th harmonic voltage distortion in the substation BJS and varying number of the harmonic filters of the SB HVDC Converter Station in-service. When the confidence range, i.e. the gap between U_{H_MIN} and U_{H_MAX}, is small, the confidence range converges to the average value U_{H_AVE}, the measured harmonic voltage distortion is in steady-state condition and time-synchronized with the grid component statuses acquired from EL-POINT and power transports from DELFIN. In Fig. 5 such steady-state periods are marked by the green arrows.

When the confidence range diverges getting a large gap off the average value U_{H_AVE}, the measured harmonic voltage distortion transits between two steady-state values and off time-synchronization with the component statuses acquired from EL-POINT and power transports from DELFIN. In Fig. 5 such off-synchronization periods are marked by the red arrows.

When the time-synchronization is valid and completed, the changes of the measured harmonic voltage magnitudes can be set in relation to switching statuses of specific grid components. The periods where the measured harmonic voltage distortion is in steady-state conditions can now be selected for development and validation of the model.

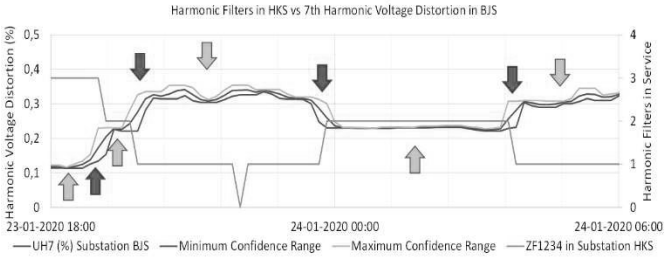

Fig. 5 Demonstration of the time-synchronization algorithm between the PQ measurements from SAFIR and the component switching from EL-POINT. The plots are: ─ average value, ─ minimum confidence range, ─maximum confidence range of the measured 7th harmonic voltage distortion in the substation BJS, and ─ number of harmonic filters in-service. The green arrows are steady-state condition and valid time-synchronization, while the red arrows mean not in steady-state and off time-synchronization.

This implies reaching an unambiguous relation between the measured (steady-state) harmonic voltage distortion in the different substations and the impedance matrix of the meshed grid according to Eq. (1-2). Therefore, the time-synchronization between the measurements of the harmonic voltage distortion and statuses of the grid components is essential for successful development and validation of the model for direct simulation of the harmonic voltage distortion.

6.2 Numerical tuning and validation

Uncertainty of the simulated harmonic distortion within the Swedish transmission grid in different operation regimes is among the largest factors which may negatively influence accuracy of the simulation model, disregarding the efforts put into the Danish part. Therefore, numerical tuning begins with determination of the harmonic distortion exchanged with the Swedish grid. The periods and snapshots with disconnected HVDC Converter Stations in Eastern Denmark are applied as the first step of numerical tuning of the harmonic emission sources, with primary focus on the HVDC Converter Stations in Sweden and the cumulative harmonic contributions behind the border substations SÅNS and MRPS. This part of numerical tuning and validation is described in subsection 6.2.1.

The simulation model shall predict both low and high magnitudes of the harmonic voltage distortion. Whether the harmonic voltage magnitudes are low or high relates to specific (n-L), $L \geq 0$, operation conditions and power transports. High magnitudes of the harmonic voltage distortion, especially when approaching and exceeding the IEC planning levels, may call for mitigation and investment decisions. Therefore, the model shall accurately simulate such high magnitudes.

The simulation model shall also accurately predict that the harmonic voltage distortion will, in given operation conditions, have low magnitudes. However, the accuracy requirement to the simulated magnitudes can be lowered meaning no need of exact match between the simulated magnitudes and low measured magnitudes of the harmonic voltage distortion.

The consecutive snapshots and simulation results where the harmonic voltage distortion changes between low and high magnitudes are presented in subsections 6.2.2 and 6.2.3.

6.2.1 Harmonic distortion exchanged with Sweden over HVAC connections: During shorter periods in Nov. 2020, both KO and SB HVDC Converter Stations in Eastern Denmark were out-of-service. These snapshots are applied for evaluation of the harmonic emission in the Swedish transmission grid on the harmonic voltage distortion in Eastern Denmark.

The snapshots are applied for numerical tuning of the harmonic emission sources in Sweden and the distributed harmonic emission sources in Eastern Denmark. Comparison of the simulated and measured magnitudes of the harmonic voltage distortion in the Danish substations with available PQ measurements is shown in Fig. 6. In the shown snapshot, the 400 kV transmission grid of Eastern Denmark is in (n-0). The harmonic voltage distortion is low meaning significantly lower than the IEC planning levels [3]. The simulations are predicting low magnitudes of the harmonic voltage distortion which is in good agreement with the PQ measurements.

The results demonstrate that the simulation model with sufficient accuracy represents the cumulative harmonic contribution of the Swedish transmission grid measured in Eastern Denmark. This is a good starting point for further numerical tuning of the harmonic emission sources of the KO and SB HVDC Converter Stations and distributed harmonic sources in Eastern Denmark.

6.2.2 Variation of 13th harmonic voltage distortion: In Aug. 2020, the grid operation led to magnitude variation of the 13th harmonic voltage distortion in the 400 kV substations HVE and ISH. In conditions with high magnitudes, the 13th harmonic voltage distortion approached the IEC planning level of 1.5% of the nominal-frequency voltage [3].

Fig. 7 shows an example among specific operation conditions in Eastern Denmark with such variation of the 13th harmonic voltage distortion between low magnitudes (marks A and C) and high magnitudes (marks B).

Fig. 8 compares the measured and simulated harmonic voltage distortion in the substations HVE and ISH with varying 13th harmonic voltage magnitudes. The simulation model predicts accurately the changes from low magnitudes in operation conditions A to high magnitudes in operation conditions B and back to low magnitudes in operation conditions C. The other harmonic orders do not show such variations of magnitudes, which is also accurately predicted by the simulation model.

The 13th harmonic distortion originates from the HVDC LCC Converter Stations. In depth analysis of the worst-case conditions anticipates that the excessive 13th harmonic voltage distortion in HVE and ISH occurred in combination of the electrical isolation of the 400 kV substation AVV, the inverter regime of the KO HVDC Converter Station close to the full power transport and two harmonic filters in-service.

For the operation conditions B with high magnitudes of the 13th harmonic voltage distortion, Fig. 9 shows the simulated coupling harmonic impedances between the substations ISH and HVE (as the first terminals) and the substations with the HVDC Converter Stations (as the second terminals). The plots in Fig. 9 do not reveal resonance conditions for the 13th harmonic order. However, the plots show that the KO, BA and SB HVDC Converter Stations can simultaneously influence the 13th harmonic distortion in ISH and HVE.

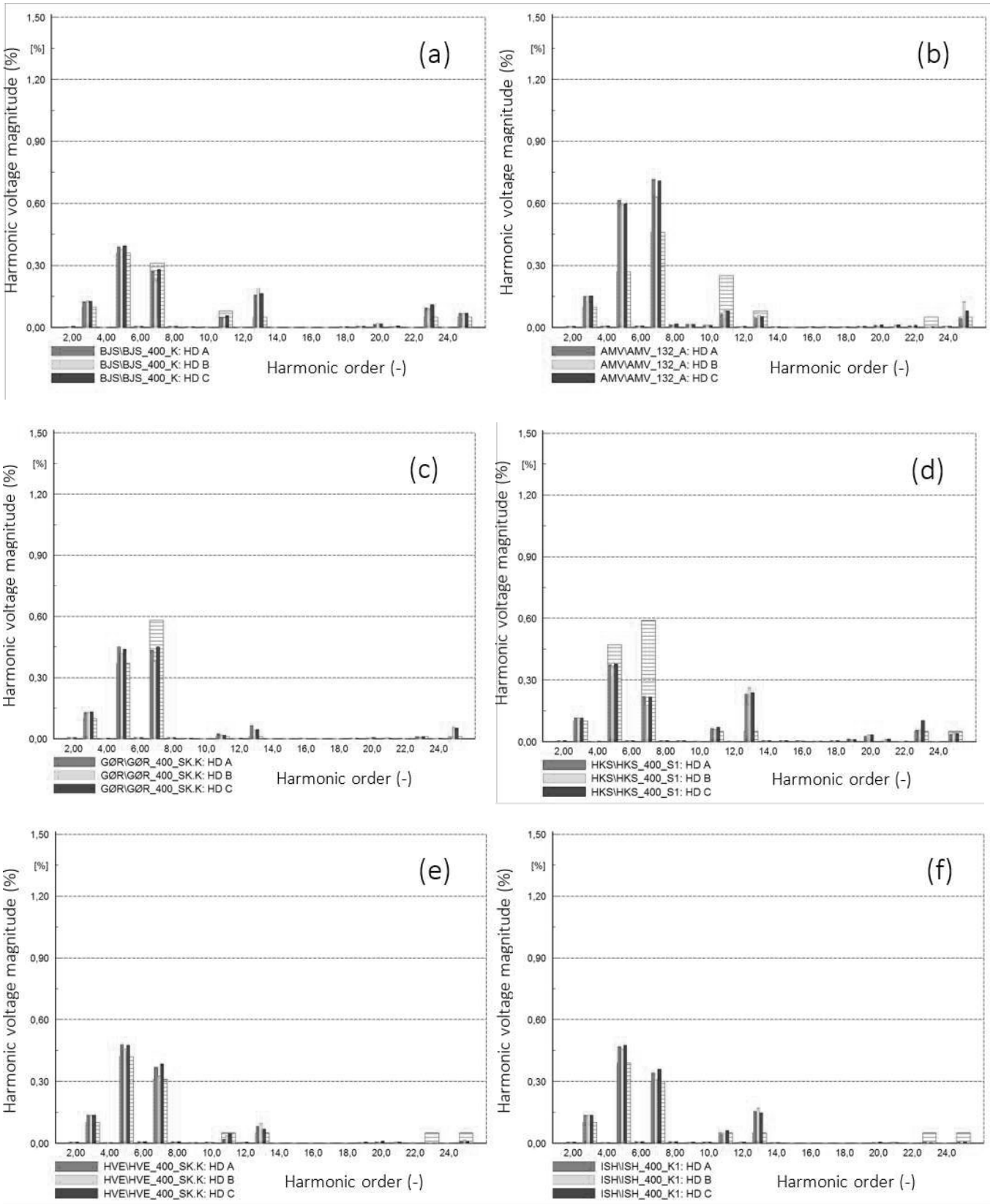

Fig. 6 Comparison of the simulated harmonic voltage magnitudes in the three phases A, B, and C marked by ▮, ▮, and ▮, to the measured harmonic voltage magnitudes marked by ▤, in the substations: (a) – BJS, (b) – AMV, (c) – GØR, (d) – HKS, (e) – HVE, (f) – ISH. The snapshot is for (*n*-0) operation conditions in Eastern Denmark and the KO and SB HVDC connections are out-of-service.

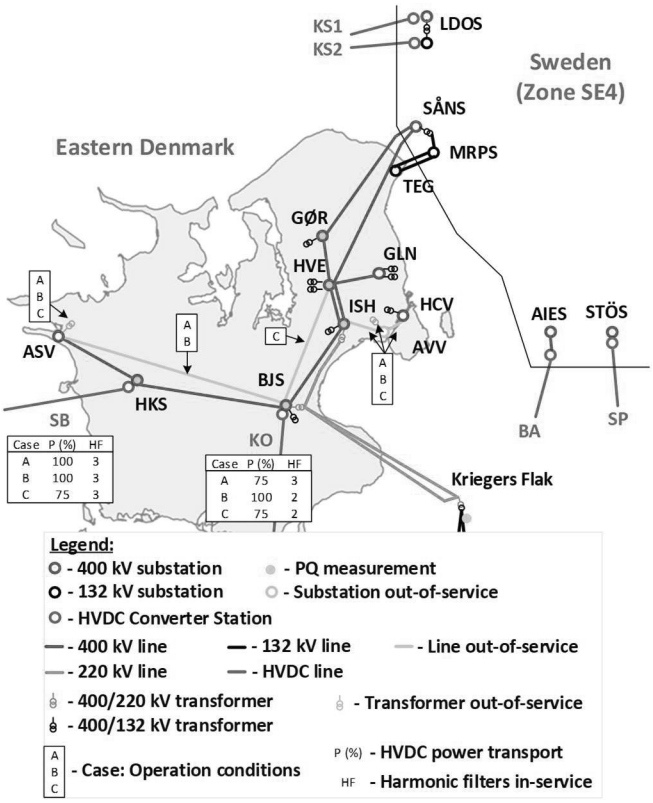

Fig. 7 Example on operation conditions in the 400 kV transmission grid of Eastern Denmark leading to variation of the 13th harmonic voltage distortion between low (marks A and C) and high (marks B) magnitudes.

A possible explanation of the high 13th harmonic voltage distortion in ISH and HVE can be that the 13th harmonic current vectors from the three above-mentioned HVDC Converter Stations reach in-phase to the substations ISH and HVE increasing the 13th harmonic voltage magnitudes in these two substations. This is the case of harmonic propagation increasing the harmonic voltage distortion in specific substations of the meshed transmission grid in certain operation conditions.

The above discussion emphasizes that representations of the harmonic emission sources is significant for accurate simulation of the harmonic voltage distortion. The harmonic propagation which may increase the harmonic voltage distortion is the result of both grid operation conditions (passive-part) and harmonic emission sources (active-part).

The given validation examples shows that the simulation model not only accurately predicts the magnitudes but also tendencies of the harmonic voltage distortion in changing operation conditions of the 400 kV meshed transmission grid.

6.2.3 Resonance shift causing high 7th harmonic voltage distortion: In July 2020, the grid operation conditions resulted in variation of the 7th harmonic voltage distortion in the 400 kV substation HKS.

The substation HKS includes the SB HVDC Converter Station and its SG, does not have 400/132 kV transformation and so does not have harmonic emission sources with significant magnitudes of the 7th harmonic order. Fig. 10 shows the operation conditions in Eastern Denmark resulting in variation of the 7th harmonic voltage distortion between low magnitudes (marks A and C) and high magnitudes (marks B).

Fig. 11 compares the measured and simulated harmonic voltage distortion in the substation HKS during varying 7th harmonic voltage magnitudes. The simulation model predicts accurately the jumps from low magnitudes in operation conditions A to high magnitudes in operation conditions B and back to low magnitudes in operation conditions C. The other harmonic orders do not show such large changes of magnitudes, which is also accurately predicted by the simulation model.

Explanation of the above-described behaviour is due to change of the harmonic impedance characteristics in the substation HKS first towards higher magnitudes of the 7th harmonic order, when the BJS-HKS line disconnects and there are two harmonic filters in-service in BJS, and then towards lower magnitudes, when a harmonic filter in BJS disconnects. Fig. 12 shows the harmonic impedance characteristics in the substation HKS confirming the above given explanation.

Attention is paid to that the harmonic filters in BJS are not tuned for the 7th harmonic order. The observed changes of the 7th harmonic voltage distortion are due to shifting of the harmonic impedance characteristics when the lines and harmonic filters are switched in- or out-of-service. This behaviour is discovered during development of the presented simulation model of the 400 kV meshed transmission grid of Eastern Denmark.

The simulation model can overestimate the 5th harmonic voltage magnitudes in the summer periods used for validation, because the 5th (and 7th) harmonic emission sources are tuned for the maximum 95th percentiles which for the 5th harmonic order are largest during the winter months (and does not have such seasonal dependency for the 7th harmonic voltage distortion).

The given validation example confirms that the simulation model accurately predicts both magnitudes and tendencies of the harmonic voltage distortion in changing operation conditions of the 400 kV transmission grid.

7 Risks and Their Mitigation

Though the presented method and simulation model are successfully validated using the PQ measurements, there are risks of uncertainty and discrepancies of the simulated harmonic voltage distortion. Uncertainties and discrepancies can be both due to inaccuracies of passive-part and active-part of the simulation model.

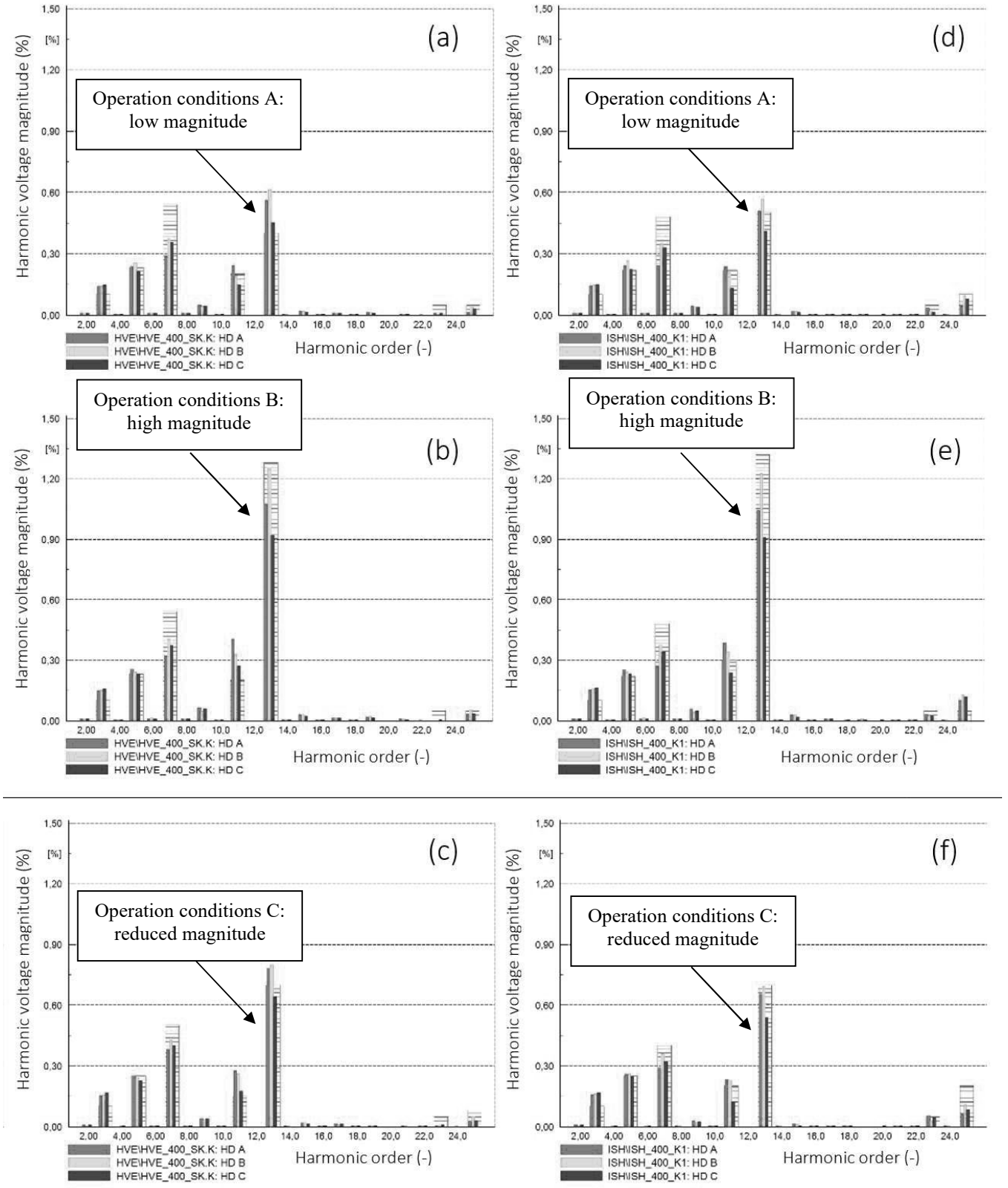

Fig. 8 Comparison of the simulated harmonic voltage magnitudes in the three phases A, B, and C marked by ▮, ▯, and ▮, to the measured harmonic voltage magnitudes marked by ☰, in the substations: (a), (b), (c) – HVE, (d), (e), (f) – ISH during the grid operation conditions leading to variation of the 13th harmonic voltage distortion between low and high magnitudes.

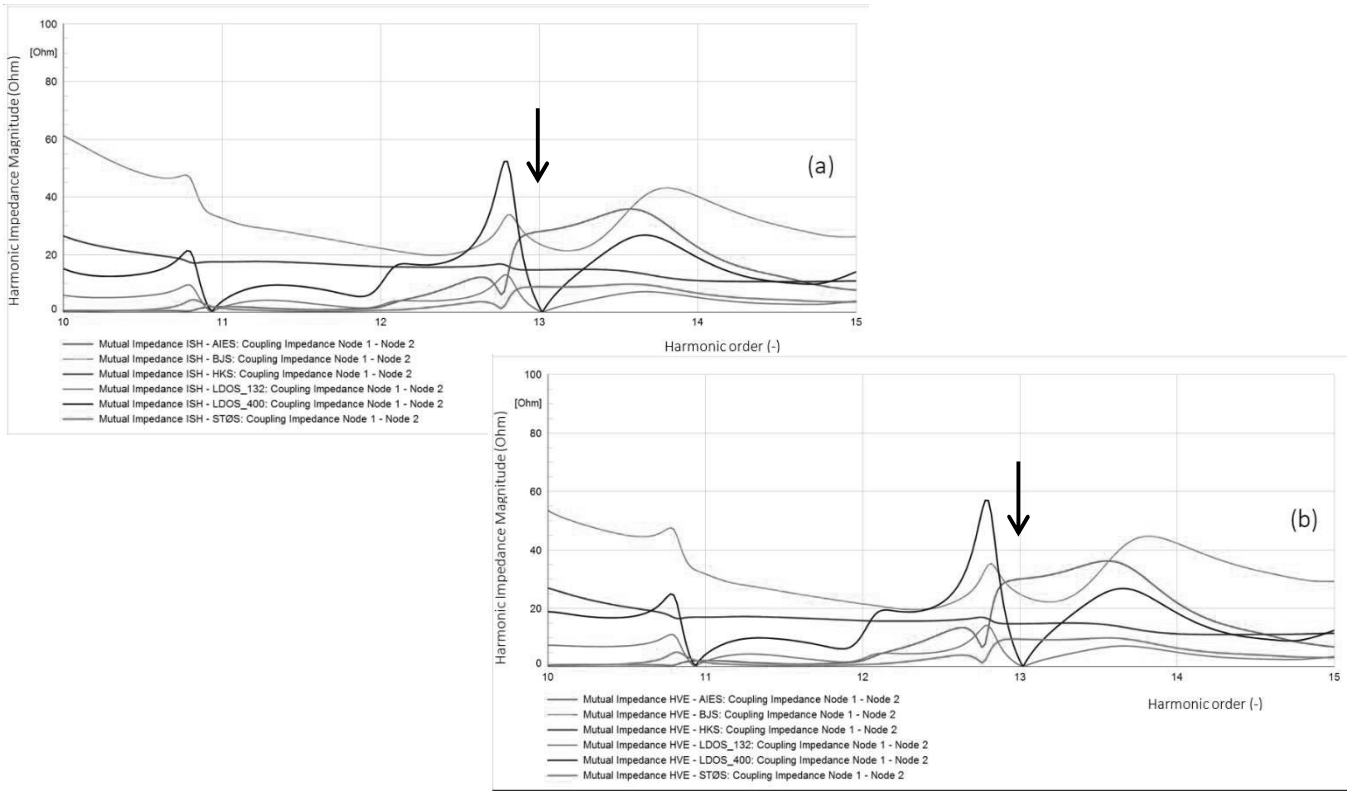

Fig. 9 Coupling harmonic impedance magnitudes between the 400 kV substation: (a) – ISH and (b) – HVE (as the first terminals), and the substations of the HVDC Converter Stations (as the second terminals): ▮ - BA (SE4), ▮ - KO (DKE), ▮ - SB (DKE), ▮ - KS2 (SE4), ▮ - KS1 (SE4), and ▮ - SP (SE4). The plots are for operation conditions B with high 13th harmonic voltage magnitudes in ISH and HVE.

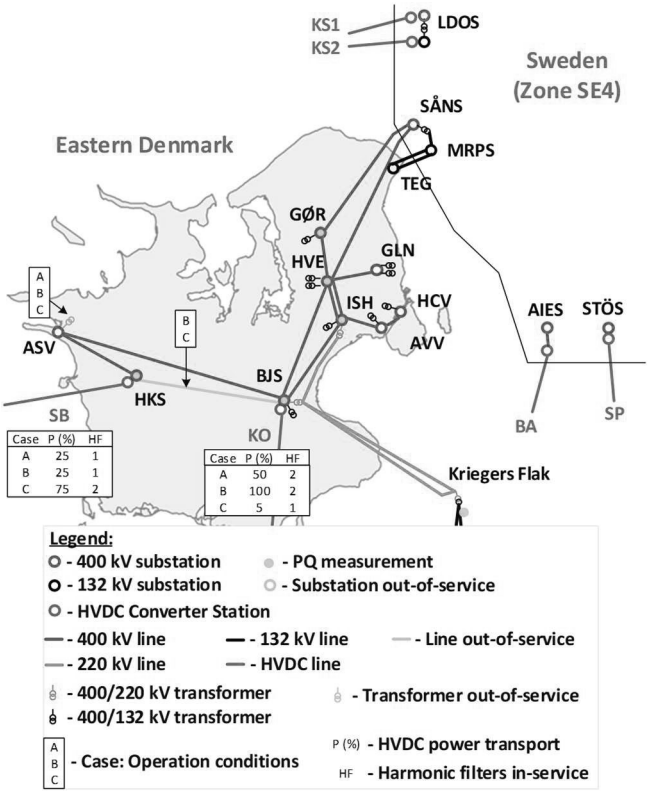

Fig. 10 Operation conditions in the 400 kV transmission grid of Eastern Denmark leading to variation of the 7th harmonic voltage distortion between low (marks A and C) and high (marks B) magnitudes.

However, the main risk of the method arises from uncertainties of the present and evolution of harmonic emission sources in the physical grid, such as new harmonic sources are added. The risks of the method shall be reduced by the following measures.

Considering the passive-part, the electro-geometrical data of the connections shall be carefully prepared and evaluated, using impedance measurements for the existing connections.

A suitable confidence margin shall be added to the simulated magnitudes of the harmonic voltage distortion when evaluating the simulation results and mitigation. The simulation results of direct simulation of the harmonic voltage distortion using harmonic load-flow shall be complemented with frequency sweeps of the harmonic impedances for the present and future transmission grid stages. The conclusion on changed harmonic voltage distortion and needs of mitigation of both methods applying direct simulation and frequency sweeps shall support each other.

The data uncertainty and unavailability of foreign grids are to be treated with all needed care and precaution when conducting harmonic assessment of the grid reconstruction and expansion projects in the domestic grid.

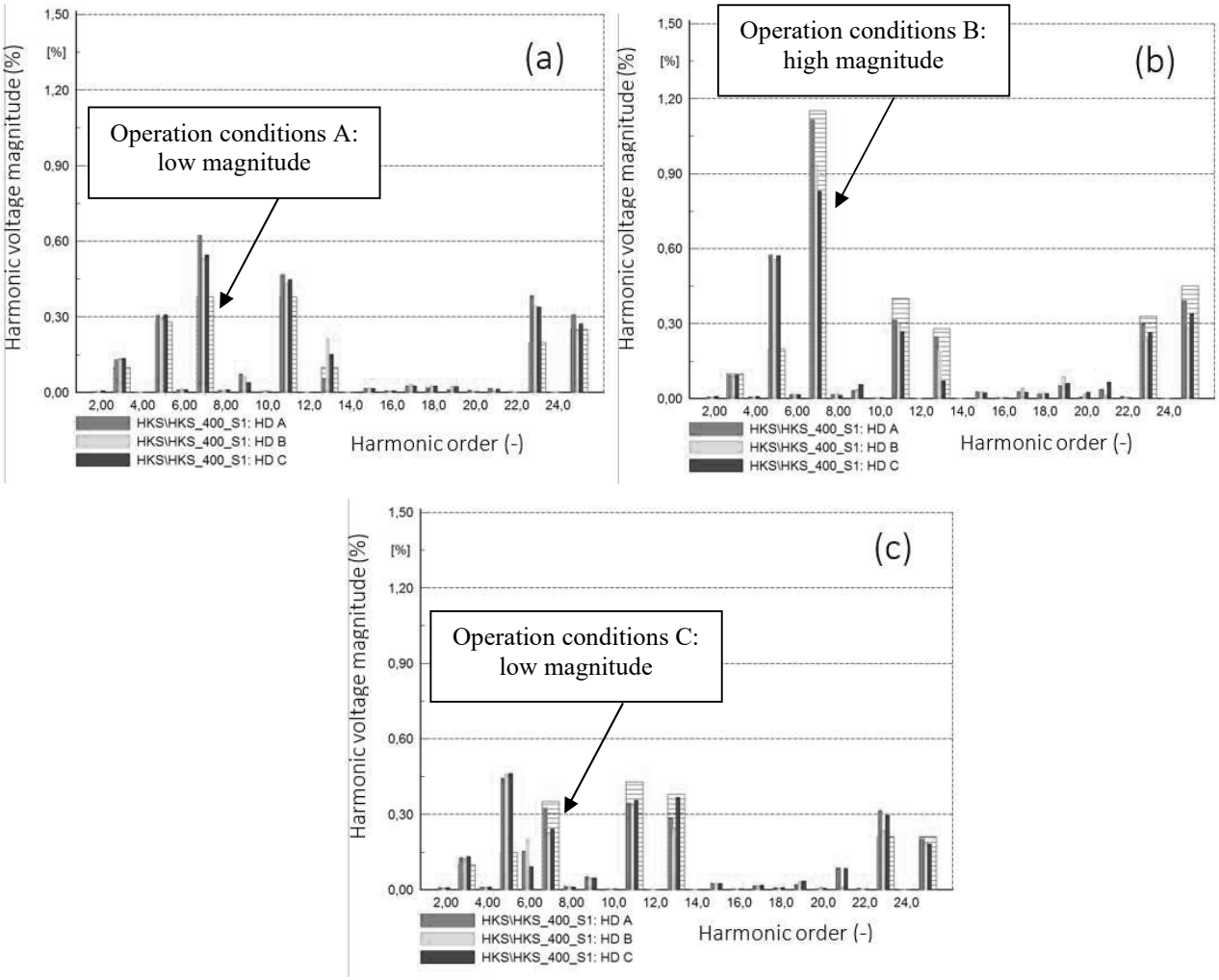

Fig. 11 Comparison of the simulated harmonic voltage magnitudes in the three phases A, B, and C marked by , , and , to the measured harmonic voltage magnitudes marked by , in the substation HKS for the operation conditions (a) - A, (b) - B, (c) - C during variation of the 7th harmonic voltage distortion between low and high magnitudes.

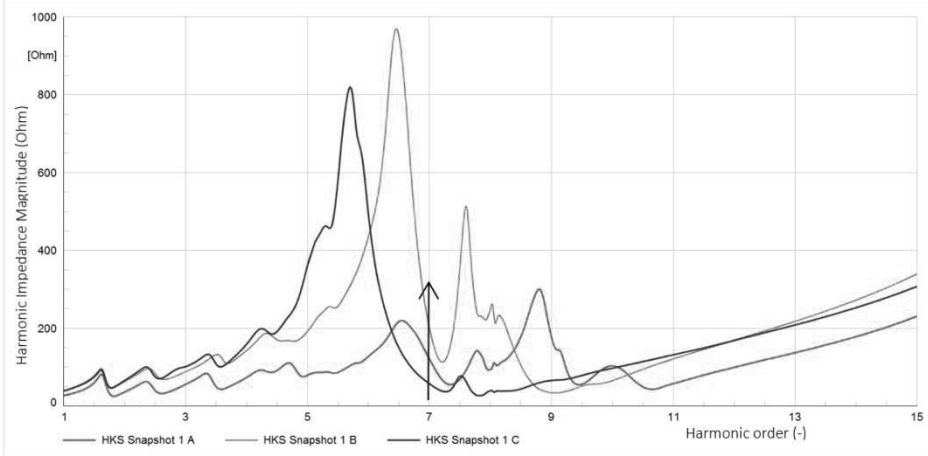

Fig. 12 Harmonic impedance magnitudes in the 400 kV substation HKS in the grid operation conditions:: - A, - B, - C.

The representations of the harmonic emission sources shall be re-evaluated and readjusted at the first given opportunity following completion of the grid development project before proceeding with harmonic assessment of the next project.

Both severity and statistical occurrence of the excessive simulated harmonic voltage distortion shall be included in the judgement of whether the grid development project results in violation of the IEC planning levels in means of the weekly 95th percentiles and/or requires mitigation solutions.

The statistical occurrence can be evaluated using the operation regimes of the present transmission grid as reference.

8 Future Trends of Harmonic Assessment

The presented method and developed simulation model allow direct simulation of the harmonic voltage distortion in the present and next development stages of a meshed transmission grid with multiple emission sources. Thus, the method allows prediction of the harmonic voltage distortion after commissioning of a grid development project.

The assessment procedure is by simulations of numerous operation scenarios which is a kind of an observational study. As many various operation scenarios are included, as better chances are for finding critical conditions resulting in excessive harmonic voltage distortion in a future grid stage.

At present, Energinet and AAU Energy, Aalborg University, are conducting an Industrial PhD project [6] with the aim of developing analytical methods to determine harmonic propagation in meshed systems. The expected outcome is that the developed methods will become a robust tool for determining the risk of changes in harmonic propagation due to changes in the transmission network and for determining most suitable filter locations in the meshed transmission grid. Some of this work has shown that harmonic propagation in the transmission network can be considered as standing waves and that these phenomena can help to bring a greater understanding of the criteria that determine harmonic propagation in meshed transmission systems [7].

It is also expected that the methods can uncover whether it is possible to make an analytically harmonic assessment instead of, or in parallel with, observational studies for focused operating scenarios, and if so, for what conditions it is possible. The term 'focused' implies a reduced number of simulation cases selected according to the analytical approach. Furthermore, the Industrial PhD project must define whether there are maximum values for the harmonic distortion that can most likely never be exceeded under given operating conditions, and how such magnitudes are determined in present and future grid development stages. Finally, the Industrial PhD project will propose methods for assessing the angular displacement of the individual harmonics when they are propagating through the grid.

9 Conclusion

The green transition of the electric energy generation and consumption as well as construction of the Energy Islands stipulates accelerated development and reconstruction of the transmission grid. In Denmark, the grid development shall for the most technically possible extent utilize the HVAC UGC instead of OHL. Increasing share of UGC has brought the resonances of the harmonic grid impedances down into the range of the harmonic emission sources, which results in the harmonic voltage distortion may substantially increase in some parts and reduces in other parts of the meshed transmission grid. Therefore, securing adequate levels of the power quality in future grid development stages and prediction methods of the harmonic voltage distortion by simulations become relevant for successful green transition.

This paper has proposed a method for direct simulation of the harmonic voltage distortion in the meshed transmission grid with numerous harmonic emission sources. In the method, different operation regimes of the transmission grid, (n-L), $L \geq 0$, represent variations of the harmonic impedance matrix of the present grid stage. The harmonic emission sources are numerically adjusted for best-possible matching the measured harmonic voltage magnitudes in different substation for the different operation regimes. The numerical tuning converges to an empirically defined solution set of the relative magnitudes and relative phase-angles of the harmonic emission sources, so that the same solution set matches the measured harmonic voltage distortion with good accuracy for most-possible operation conditions in the meshed transmission grid.

Representing the grid development projects as (n-L_1+L_2) with L_1 being the number of removed connections and L_2 the added connections and applying the solution set with locked relative magnitudes and phase-angles of the harmonic emission sources, the proposed method can simulate the harmonic voltage distortion in a future grid.

The primary goal has been that the method predicts whether, how severely and where in the transmission grid, the harmonic voltage distortion is going to increase and needs mitigation after the grid development projects (n-L_1+L_2). Therefore, the method simulates accurately high magnitudes of the harmonic voltage distortion because high magnitudes may need mitigation. The method also predicts accurately but does not necessarily exactly match low magnitudes of the harmonic voltage distortion.

The method has been illustrated using a simulation model of the 400 kV transmission grid of Eastern Denmark. Accuracy of the model with numerically adjusted magnitudes and phase-angles of the harmonic emission sources has been confirmed by validation using the PQ measurements. The validation included not only static magnitudes in “frozen” operation conditions of the grid but also change tendencies of the harmonic voltage distortion following changes of the grid operation conditions.

The method is deterministic and subject to uncertainties influencing accuracy of the simulated harmonic voltage distortion. Such uncertainties include both tolerances of the grid data, measurements applied for the model setup and representation of the harmonic emission sources. Therefore, the simulation model shall be revalidated and, when deemed necessary, recalibrated after establishment of new passive-grid components and new harmonic sources.

The development trend is substitution of many simulations (observational studies) by less focused simulations and optimal mitigation using analytical methods.

10 References

[1] Akhmatov, V., Hansen, C. S., Jakobsen, T.: 'Development of a harmonic analysis model for a meshed transmission grid with multiple harmonic emission sources', Paper WIW20-39, 19th Wind Integration Workshops, Nov. 11-12, 2020, Virtual Conference.

[2] Akhmatov, V., Hansen, C. S., Jakobsen, T.: 'Methods and results of harmonic simulation assessment of a reconstructed meshed transmission Grid with distributed harmonic emission sources', Paper WIW21-10, 20th Wind Integration Workshops, 29-30 Sept. 2021, Berlin, Germany.

[3] IEC 61000-3-6: 'Electromagnetic Compatibility (EMC) – Part 3-6: Limits – Assessment of emission limits for the connection of distorting installations to MV, HV and EHV power systems'.

[4] Kwon, J. B.: 'System-wide amplification of background harmonics due to the integration of high voltage power cables', Paper C4-305, CIGRÉ Session 2020.

[5] Akhmatov, V., Sørensen, M., Jakobsen, T., Hansen, C. S., Gellert, B. C., Bukh, B. S.: 'Design algorithm of harmonic filters in a meshed transmission grid with distributed harmonic emission – Eastern Danish transmission grid case study', Paper WIW22-5, 21th Wind and Solar Integration Workshops, Oct. 12-14, 2022, Delft, The Netherlands.

[6] Bukh, B. S.: 'Methods for harmonic analysis in meshed transmission systems.' [Online]. Available: https://vbn.aau.dk /en/projects/methods-for-harmonic-analysis-in-meshed-transmission-systems, accessed 24 May 2022.

[7] Bukh, B. S., Bak, C. L., Faria da Silva, F.: 'Analysis of harmonic propagation in meshed power systems using standing waves', Paper C4-563, CIGRÉ Session 2022.

Appendix A – Harmonic Simulation of Vejle-Ådal

In July 2017, a section of the 400 kV OHL line between the substations Landerupgård and Malling, at Vejle-Ådal in Western Denmark, is replaced with a 7 km double 400 kV UGC, see Fig. 1. After energization of the 400 kV UGC, a significant increase of the 11th harmonic voltage distortion is measured in the 400 kV substations Trige and Fraugde, while the harmonic distortion in other 400 kV substations remained almost unchanged. The measured 11th harmonic distortion in the substations Trige, Fraugde and V. Hassing is shown in Fig. 13.

Using the presented method, the Vejle-Ådal UGC influence on the harmonic voltage distortion in Western Denmark is evaluated. The assessment procedure has been:

- The parameters of the harmonic source models of the HVDC Converter Stations in Fraugde, V. Hassing, Tjele and the Anholt wind power plant, are set for the grid stage after commissioning of the Vejle-Ådal UGC [1], locked and kept unchanged.
- Simulations using the grid stage model after commissioning of the Vejle-Ådal UGC are carried out.
- In the grid model, the Vejle-Ådal UGC is replaced with the OHL section (reversing the grid stage to before the Vejle-Ådal UGC). Simulations are now carried out using the same parameters of the harmonic source models.

The simulation results of the 11th harmonic voltage magnitudes before and after the Vejle-Ådal UGC are shown in Fig. 14. The simulation results are in good agreement with the measurements in Fig. 13, accurately predicting increase of the 11th harmonic distortion in Trige and Fraugde and no such increase in V. Hassing due to the Vejle-Ådal UGC.

The Vejle-Ådal UGC causes unbalanced amplification of the 11th harmonic distortion in Trige, which is evident from analysis of the harmonic voltage magnitudes in the three phases shown in Fig. 13. Therefore, application of electro-geometrical distributed line models of OHL and UGC and frequency-dependent network equivalents for the positive-, negative- and zero-sequences are among preconditions of successful evaluation of the presented case.

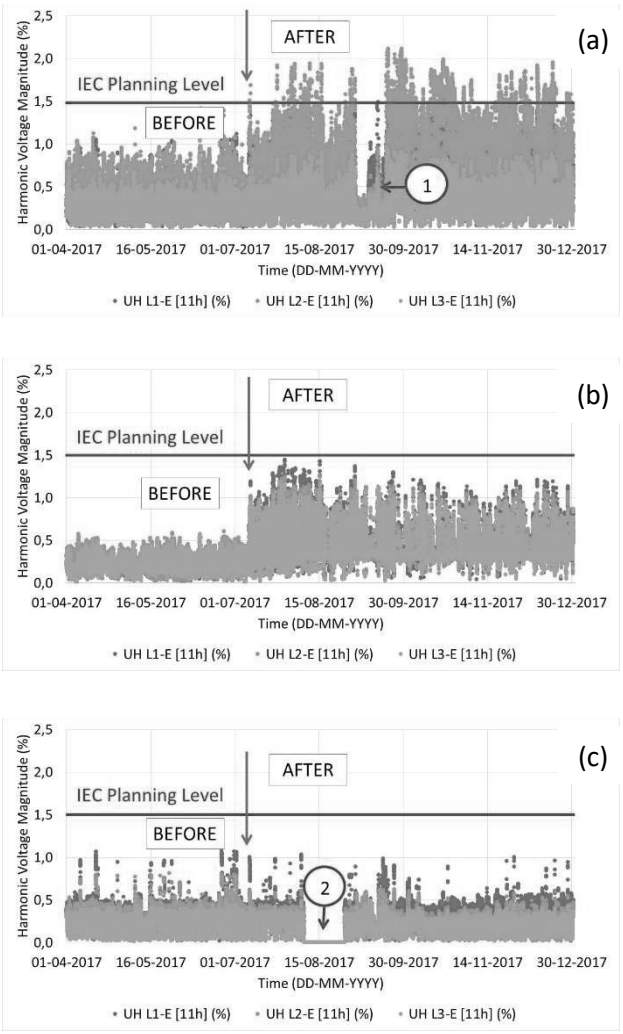

Fig. 13 Measured 11th harmonic voltage distortion in the three phases before and after commissioning of the Vejle-Ådal UGC in the substations: (a) – Trige, (b) – Fraugde, (c) – V. Hassing. The substations in Denmark are shown in Fig. 1. The blue arrow marks the commissioning time, and the marks are: 1 – KS1 and KS2 HVDC are out-of-service and (*n*-1) in the grid, 2 – PQ measurement is not available due to (*n*-1) in the grid.

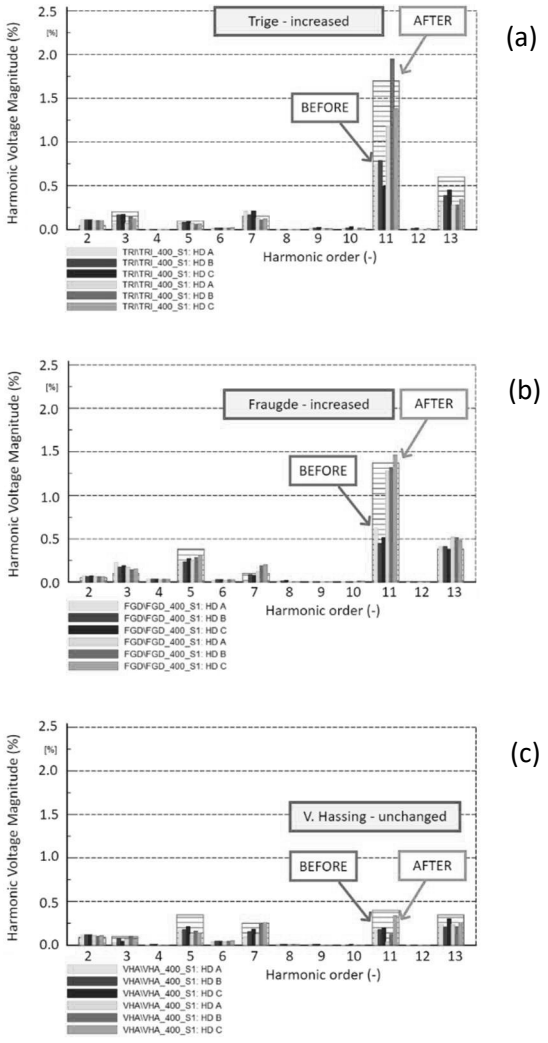

Fig. 14 Simulated harmonic voltage distortion in the three phases before and after commissioning of the Vejle-Ådal UGC in the substations: (a) – Trige, (b) – Fraugde, (c) – V. Hassing. The substations in Denmark are shown in Fig. 1. The color marks are: **blue** – simulation before, **green** – simulation after, **red boxes** – measurement after energization of the Vejle-Ådal UGC.